

# Fabrication and *in vitro* evaluation of pH/thermo dual responsive hydrogels as controlled ibuprofen sodium *in situ* depot

Samiullah Khan<sup>a</sup>, Abdur Rehman<sup>b</sup>, Syed Faisal Badshah<sup>c</sup>, Gamal A. Shazly<sup>d</sup>, Amira Metouekel<sup>e</sup> and Fakhreldeen Dabiellil<sup>f</sup>

<sup>a</sup>College of Pharmacy, Margalla Institute of Health Sciences, Islamabad, Pakistan; <sup>b</sup>College of Pharmaceutical Sciences, Soochow University, Suzhou, China; <sup>c</sup>Department of Pharmacy, Faculty of Medical and Health Sciences, University of Poonch Rawalakot, Azad Jammu and Kashmir, Pakistan; <sup>d</sup>Department of Pharmaceutics, College of Pharmacy, King Saud University, Riyadh, Saudi Arabia; <sup>e</sup>University of Technology of Compiègne, Compiègne Cedex, France; <sup>f</sup>University of Bahr el Ghazal, Wau, South Sudan

## ABSTRACT

Ibuprofen sodium (IBP) is a commonly used NSAID for multiple pain conditions. However, despite its extensive use, it is associated with multiple GIT adverse effects after oral administration. In the present study, we have fabricated thermoresponsive gel depot using Poly (N-vinylcaprolactam) and sodium alginate as polymers. The designed formulations are intended to be used as IBP depot after being administered subcutaneously. The sol-gel phase transition temperature and gelation time of gel samples were optimized by tube inversion, rheological exploration and optical transmittances. Temperature sweep experiments confirmed that optimized gel samples have sol-gel transition between 32°C and 37°C. Swelling and *in vitro* drug release displayed that optimized gels have maximum swelling and IBP release at pH 7.4 and at 35°C confirming their pH/thermo sensitivity. The degradation profile of hydrogels displayed controlled degradation for 6 days that with increasing contents. MTT assay showed L929 cells displayed more than 90% cell viability against blank and IBP-loaded PNVCL/NaAlg hydrogels at optimized concentrations. Fourier transform infrared spectroscopy confirmed the polymer blend hydrogels structure formation. Thermogravimetric analysis confirmed the presence of thermoresponsive moieties and thermal stability of polymer blend hydrogel sample. While scanning electron microscopy showed that hydrogel has channels in structure that might facilitate the diffusion of solvent. Results concluded that PNVCL/NaAlg hydrogels can be utilized as IBP sustained depot following subcutaneous application *in vivo* and GIT adverse effects could be avoided associated with its oral administration.

## ARTICLE HISTORY

Received 27 August 2024  
Accepted 9 December 2024

## KEYWORDS





Thermogels; Poly (N-vinylcaprolactam); sodium alginate; *in situ* depot; rheology; MTT assay

## 1. Introduction

Hydrogels belong to biomaterials with a three-dimensional structure. Their most significant feature is their capacity to swell and shrink as soon as any biological medium or swelling diffuse into or effuse out of the network [1]. Environmentally responsive hydrogels, which have the capability to respond to external or internal stimuli, have drawn a lot of attention in course of sustained release carriers [2,3]. Intelligent monomers or polymers from which hydrogels are being formulated respond primarily to stimuli such as temperature, light, pH, electric and magnetic fields, ionic strength and salt nature. Because of having such intelligence qualities, these stimuli responsive formulations are frequently referred to as 'materials with brains.' These responsive formulations closely resemble physiological processes that occur naturally, whereby changes in physiological

state can regulate the release of the therapeutic agents that have been encapsulated [4,5].

Researchers working on biomaterials are currently shifting their attention to injectable biodegradable *insitu* hydrogels, having potential to be used in drug delivery, tissue engineering and means of delivering proteins. Injectable *insitu* formed hydrogels, which are easy to formulate, have a higher loading capacity and are easier to apply as controlled delivery depots. They exist in solution phase at room temperature and change into gel form in response to body temperature. *Insitu* formed injectable hydrogels are particularly interesting for drug delivery because they don't need to be surgically implanted like premade sustained-release implants do, and they only need to be injected for *in vivo* depot development. The ability of injectable hydrogels to adapt to the shape of

**CONTACT** Samiullah Khan  [Sami\\_pharmacist99@hotmail.com](mailto:Sami_pharmacist99@hotmail.com)  College of Pharmacy, Margalla Institute of Health Sciences, Islamabad, Pakistan; Fakhreldeen Dabiellil  [researcherzem@gmail.com](mailto:researcherzem@gmail.com)  University of Bahr el Ghazal, Wau, South Sudan

© 2024 The Author(s). Published by Informa UK Limited, trading as Taylor & Francis Group.

This is an Open Access article distributed under the terms of the Creative Commons Attribution-NonCommercial License (<http://creativecommons.org/licenses/by-nc/4.0/>), which permits unrestricted non-commercial use, distribution, and reproduction in any medium, provided the original work is properly cited. The terms on which this article has been published allow the posting of the Accepted Manuscript in a repository by the author(s) or with their consent.

tissues and deliver medications or cells in a less invasive way makes them advantageous for macrophage migration, proliferation, and differentiation [6–8].

When injected into the body, these *insitu* sol-gel transition hydrogels, based on temperature-responsive polymers, form *insitu* depots at body temperature and allow the sustained release of loaded compounds. Majority of polymers generally exhibit aqueous solubility on heating; nevertheless, many water soluble polymers precipitate out of solution. This property called lower critical solution temperature (LCST) is shown by class of polymers which solubilize upon cooling and undergo phase separation upon heating [9]. Water molecules stay bonded to the network chain below the LCST in the hydrophilic state. Above LCST, however, hydrophobic interactions become dominant and lead to the release of water moieties from the network series [10]. Temperature-sensitive materials like poloxamers (Pluronic), poly (ethylene glycol), poly (N-isopropylacrylamide), poly (ethylene oxide), and N-vinylcaprolactam are typically employed in fabrication of thermoresponsive *insitu* produced gels [11,12].

N-Vinylcaprolactam (NVCL) is a amphiphilic material containing carboxylic (hydrophilic) and vinyl (hydrophobic) groups, possessing nonionic, temperature-sensitivity, biocompatible and nontoxic properties. NVCL has LCST in the physiological temperature range (32–37°C), which made it a suitable ingredient for pharmaceutical products [12,13]. The molecular weight and monomer concentration of the NVCL are directly correlated with its LCST [14]. Because of their water solubility, biocompatibility, lack of adhesiveness and reversal thermoresponsive activity close to body temperature, NVCL formulations have drawn scientists' interest [12,15].

Polysaccharide polymers being nontoxic, biocompatible, less costly, biodegradable and readily available have been widely utilized in fabrication of controlled *insitu* drug delivery depots. Because of its ability to form gel, sodium alginate (NaAlg) is a naturally occurring polymer which is renewable, biocompatible and biodegradable with a wide range of commercial uses. Alginates are anionic linear polysaccharides consisting of  $\alpha$ -L-guluronate and  $\beta$ -D-mannuronic acid residues originating from natural sources and belonging to the Phaeophyceae family. Due to their non-toxic properties, alginates and their derivatives are frequently utilized in food, cosmetics and formulation of drug delivery systems [12,16,17].

Hydrophobic drugs have low water solubility, leading to poor bioavailability at absorption sites after being administered orally which diminishes their therapeutic effect. NSAIDs, such as ibuprofen sodium

(IBP), 2-(4-isobutylphenyl) propanoic acid, are commonly used to treat osteoarthritis, rheumatoid arthritis, dental pain, musculoskeletal pain and other various pain disorders [18]. Ibuprofen reduces the production of prostaglandin and thromboxanes by blocking the activity of cyclo-oxygenase I and II. This results in a reduction of prostaglandin synthesis via prostaglandin synthase, which is the primary physiological impact of ibuprofen. Despite the fact that IBP has shown therapeutic benefits, 90% of users are at an elevated risk of gastrointestinal problems, such as gastric ulcers, bleeding from the stomach mucosa, urine failure and cardiovascular effects. Therefore, developing novel drug carriers with sustained release nature is essential for providing controlled release of IBP and reduction of associated side effects [19].

With a new approach that can sustain the drug release, injectable *insitu* gelling depot delivery system may help patients to recover directly from their pain by increasing patient compliance, efficiency and reducing the harmful effects of the drugs on other tissues and organs. Herein, we report the formation of NVCL-based *insitu* forming thermoresponsive depot injectable hydrogels with polysaccharide (sodium alginate) for sustained delivery of IBP. Cold method was adopted for the design of series of *insitu* forming hydrogels. The sol-gel transition temperatures and gelation time of hydrogel samples were optimized by studying their rheological profile and optical transmittance measurement. The effect of pH and temperature on swelling profile of hydrogels was examined across different pH levels and varying temperatures. Additionally, hydrogel samples were screened for drug contents analysis and *invitro* release study at varied pH and temperatures using Franz diffusion cells. The biocompatibility of *insitu* dual responsive hydrogels was assessed using the methyl thiazolyl tetrazolium assay on L929 (mouse fibroblast cell lines). The hydrogel structure formation and thermal properties were evaluated using Fourier transform infrared spectroscopy (FTIR) and thermogravimetric analysis (TGA). The morphology of the formed depot hydrogels was examined using scanning electron microscopy (SEM).

## 2. Materials and methods

### 2.1. Materials

Sodium Alginate (NaAlg) (MW = 10000–600000 Da) was purchased from Sigma Aldrich. N-(Vinylcaprolactam, MW = 139.19 g/mol) (98%, Sigma Aldrich) stored at 4°C. Ibuprofen sodium (IBP, Purity = 99.97%). Ammonium

persulfate, sodium hydroxide, sodium chloride and acetic acid were used as analytical reagents. All chemicals were used as received without further processing.

## 2.2. Synthesis of IBP loaded poly (N-vinylcaprolactam)/sodium alginate (PNVCL/NaAlg) thermoresponsive hydrogels

The hydrogel samples were synthesized using a cold method. Initially, NaAlg was dissolved in distilled water at 600 rpm for 30 minutes according to the feed ratio specified in Table 1. NVCL was then dissolved in cold distilled water for 20 minutes and stored at 4°C until a clear solution was obtained. NVCL solution was slowly added to the previously prepared NaAlg solution with constant stirring. Ammonium persulfate was then incorporated to the polymer blend solution, and kept on stirring for 1 hour to initiate polymer blending. For the preparation of IBP loaded samples, IBP (200 µg/ml) was incorporated to final polymer blend solution under stirring. Finally after complete mixing, polymer blend mixture was filtered (0.22 micron) and screened for rheological analysis and phase transition temperature (Tsol-gel) [12,20,21]. Samples with Tsol-gel between 32°C and 37°C were optimized and used for further studies.

## 2.3. Clarity of PNVCL/NaAlg hydrogels

The hydrogel solutions and synthesized gels samples were screened visually for clarity analysis at diverse temperatures i.e., 4°C, 25°C and 37°C.

## 2.4. Phase inversion determinations

The phase inversion temperature (Tsol-gel) of each sample formulation was determined using the tube titling method [22]. Five milliliter aliquots of each formulation listed in Table 1 were moved to a glass vial and sealed with parafilm. Glass vial was kept in digital water bath at 20°C. On each occasion, sample was heated gradually at 1°C/min rate from 20°C until reaching the temperature at which sample ceased moving when tilted at a 90° angle. The same technique was applied to determine the

gelation time (Tg) of hydrogel samples. In short, a glass vial (10 ml) containing the hydrogel solution (5 ml) was inserted in water bath set at 32°C, and time calculation was started. By tilting the tubes, the sample flow nature was measured after every 10 seconds. The gelation time was measured by stopping the sample flow, and the results were noted [12,22].

## 2.5. Rheological analysis

The rheological characteristics of optimized PNVCL/NaAlg thermoresponsive hydrogels were measured using AR2000 rheometer by conducting various rheological tests.

Time sweep measurements were conducted at 30°C with a constant oscillation frequency of 1 rad/s to examine rheological characteristics. Viscoelastic qualities that are dependent on temperature were observed by temperature sweep tests, wherein temperature of circulating water bath equipped with a rheometer was varied between 25°C and 40°C at 2°C per minute heating rate. In oscillation mode, impact of temperature on viscosity measurement, storage modulus (G') and loss modulus (G'') was assessed at 1 rad/s frequency and 0.1 Pa shear rate. In a flow mode, viscosity change was monitored under shearing rate of 0.1–10 s<sup>-1</sup> [2,22].

## 2.6. In vitro degradation analysis

The weight loss analysis was used to define the *invitro* degradation of PNVCL/NaAlg hydrogels. Every hydrogel sample was first weighed (W<sub>0</sub>) and then put into 10 ml glass tube containing PBS (pH = 7.4, 5 ml). The glass tubes were kept in a shaking incubator at 37°C required time, with continuous PBS replenishment at 400 rpm. Samples were frozen rapidly at -80°C each time, lyophilized and again weighed (W<sub>t</sub>) at predetermined intervals. Weight loss ratio was measured by following formula [5,23];

$$\text{Weight Loss(\%)} = \frac{W_0 - W_t}{W_0} \times 100$$

Where W<sub>0</sub> and W<sub>t</sub> indicate sample weights prior and post degradation respectively.

**Table 1.** Feed composition, tsol-gel and tg of pH/thermo dual responsive PNVCL/NaAlg hydrogels.

Formulations	PNVCL (g)	NaAlg (g)	APS (g)	T <sub>sol-gels</sub> (°C)	Gelation Time (T <sub>g</sub> ) (Mints)	IBP (mg)	Distilled Water (g)
VNa-1	0.5	0.075	0.050	40 ± 0.30	–	–	QS to 10 g
VNa-2	1	0.075	0.050	36 ± 0.40	~9	–	QS to 10 g
VNa-3	1	0.100	0.050	37 ± 0.10	~11	–	QS to 10 g
VNa-4	1.50	0.075	0.050	36 ± 0.30	~7.5	0.020	QS to 10 g
VNa-5	2.00	0.075	0.050	34 ± 0.30	~5	0.020	QS to 10 g
VNa-6	2.50	0.075	0.050	32 ± 0.20	~3.5	0.020	QS to 10 g

## 2.7. Swelling profile analysis

The swelling profile analysis of PNVCL/NaAlg pH/thermo-responsive hydrogels were performed in sealed containers with PBS (pH 7.4) and (1.2, 0.1 M HCl) at 35°C and 40°C. Samples with a specified weight were submerged in 50 milliliters of media and placed at an appropriate temperature in a water bath. Beaker was sealed with parafilm to prevent the flow of solvent out of the beaker. After specific time interval, buffer solution was removed and the gel surface was cleaned with paper to remove any surface liquid. Then the sample was weighed and reverted back to beaker [12,24]. The swelling percentage was determined by following equation;

$$\text{Swelling Ratio \% (SR)} = \frac{W_s - W_d}{W_d} \times 100 \quad (1)$$

Where  $W_s$  shows swollen samples weight and  $W_d$  shows dry samples weight respectively.

## 2.8. Optical transmittance analysis

PNVCL/NaAlg hydrogel samples' optical transmittances were determined at various temperatures using UV-Visible spectrophotometer at 450 nm. Measurements were taken using disposable cuvettes in a digital water bath. Every sample was held for 5 minutes prior to transmittance investigation under 25°C to 45°C temperature [5,25].

## 2.9. Drug contents retrieved

Co-polymer hydrogel solution (5 ml) containing IBP (200 ug/ml) was allowed to gel in a glass vial kept at 35°C in a water bath. The extracted solvent, 5 ml (PBS), was added after gelation, parafilm sealed, and kept in a water bath for 24 hours. After 24 hours, the solvent was withdrawn and processed for determination of drug contents using a UV-1601 spectrophotometer (Shimadzu) at 220 nm. The following formula was used for the determination of the drug contents [3,26];

$$\text{Drug loading \%} = \frac{W_T - W_e}{W_T} \times 100 \quad (2)$$

Where  $W_T$  denotes the total drug contents in a sample and  $W_e$  specifies the drug contents in supernatant.

## 2.10. In vitro drug release

Franz cells were used to determine the *invitro* IBP release from PNVCL/NaAlg hydrogel samples. Optimized IBP-loaded PNVCL/NaAlg hydrogel samples were placed in donor compartment with permeation

area of 0.800 cm<sup>2</sup>. The co-polymer solution was constantly agitated at 100 rpm and allowed to equilibrate until gelation at 37 ± 2°C. The receptor compartment was loaded with dissolution media i.e., PBS (7.4) and pH = 1.2. As long as the formulation was intact, aliquots were collected at predetermined time intervals. To maintain sink conditions, withdrawn aliquots were replaced with fresh solvent (2 ml). The samples were evaluated for drug contents *via* UV-1601 spectrophotometer at 220 nm [3,12].

## 2.11. Drug release kinetics

The data obtained from in vitro experiments was fitted to various mathematical models to assess the drug release kinetics.

### 2.11.1. Zero model

$$Q_t = Q_0 + K_0 t$$

Where  $Q_t$  is the amount of drug dissolved in time  $t$ ,  $Q_0$  is the initial amount of drug in the solution and  $K_0$  is zero order release constant.

### 2.11.2. First model

$$\ln M_t = -k_1 t + \ln M_0$$

$M_0$  is the initial amount of drug and  $M_t$  is the remaining amount of drug at time  $t$  and  $k_1$  is the first order rate constant.

### 2.11.3. Higuchi model

$$M = k_H t^{1/2}$$

Where  $M$  is the amount released at time  $t$  and  $K_H$  is the Higuchi rate equation

### 2.11.4. Korsmeyer – Peppas model

$$\ln(M_t/M_\infty) = \ln k_p + n \ln t$$

$(M_t/M_\infty)$  is the fraction of drug released at time  $t$  and  $n$  is the slope.

## 2.12. Cells culture conditions

L929 (mouse fibroblast cell lines) were cultured in Dulbecco's Minimum Essential Medium (DMEM) containing RPMI-1640, supplemented with 10% fetal bovine serum (FBS), 100 U/mL penicillin, 2 mm L-glutamine, and 100 µg/mL streptomycin. Once, 90% of the cells were confluent, cells pallets (10000 cells/well) were collected after trypsinization, centrifuged for 5minutes at 500 rpm and then placed in growth medium.

### 2.12.1. Methyl thiazolyl tetrazolium (MTT) assay

The MTT assay was used to determine the cytocompatibility of PNVCL/NaAlg hydrogels against L929 cells as per protocol. The previously cultivated cells were seeded in 96-well plates and incubated for 24 hours at  $37 \pm 1^\circ\text{C}$ . They were treated with  $100 \mu\text{l}$  of serum free medium containing blank and IBP loaded PNVCL/NaAlg hydrogels at optimized concentrations (600  $\mu\text{m}$ , 550  $\mu\text{m}$ , 500  $\mu\text{m}$ , 400  $\mu\text{m}$ , 300  $\mu\text{m}$ ) for 24 hours incubated at  $37 \pm 2^\circ\text{C}$  during which samples undergoes phase transition from solution to gels phase. Untreated cells were used as negative control, while cells treated with Triton X-100 served as positive control. Absorbance was calculated at 490 nm via Bio-Rad 680 microplate reader. Cells viability (%) was calculated according to the following equation [12,27,28];

$$\text{Cells Viability \%} = \frac{A_{\text{sample}}}{A_{\text{control}}} \times 100 \quad (3)$$

Here,  $A_{\text{sample}}$  and  $A_{\text{control}}$  shows absorbance's of sample and control wells.

### 2.13. FTIR spectroscopic analysis

Hydrogels structural confirmation was done by FTIR spectroscopy. The FTIR spectra of pure contents and freeze-dried gel samples were obtained from  $4000$  to  $600 \text{ cm}^{-1}$  using FTIR Accutrac FT/IR-4100 Series [29,30].

### 2.14. TG analysis

Thermogravimetric analyzer (DTG 500, Shimadzu) was utilized to test thermal characteristics of pure contents and fabricated hydrogels. TGA decomposition thermograms were recorded under nitrogen gas purging of  $30 \text{ ml min}^{-1}$  flow rate and  $25^\circ\text{C}$  to  $300^\circ\text{C}$  at  $10^\circ\text{C/min}$  [12,31].

### 2.15. Scanning electron microscopy (SEM)

SEM (JSM-6490A) was used to assess the structural morphologies of freeze-dried PNVCL/NaAlg hydrogel samples. On an aluminum stub, hydrogel samples were placed and coated with gold sputter. The porosity of the hydrogel was assessed by photomicrographing at 20 KV [3,12,32].

### 2.16. Statistical analysis

Results were presented as percentages or as mean  $\pm$  standard deviation (SD). Significance was evaluated

using ANOVA with GraphPad or Origin software, with a significance level at  $p < 0.05$ .

## 3. Results and discussion

### 3.1. Hydrogels clarity

Co-polymeric solutions and optimized PNVCL/NaAlg thermoresponsive hydrogel were visually observed and were found clear and transparent at  $4^\circ\text{C}$ ,  $25^\circ\text{C}$  and  $37^\circ\text{C}$ . Table 2 refers to hydrogel sample clarity.

### 3.2. Hydrogels phase transitions

The two most important variables for *in situ* forming depot formulations are gelation temperature (Tsol-gels) and gelation time (Tg). Titling method was used to determine the formulations' Tso-gels and Tg. Tso-gels of the optimized gel samples were found to be at the body temperature range ( $32\text{--}37^\circ\text{C}$ ) based on the observed results. Table 1 indicates the feed composition, sol-gel transition temperatures, and gelation time of optimized PNVCL/NaAlg thermoresponsive hydrogels. The possible mechanism behind the gelation of PNVCL/NaAlg hydrogels is the interaction between the hydrophilic -OH groups of the NaAlg chain and the carbon backbone hydrophobic chains of PNVCL. The gelation process was initiated by the incorporation of ammonium persulfate as an initiator. When a free radical initiator is present, the reactive hydroxyl groups function as potent radicals that react with vinyl groups. Furthermore, an increase in Tso-gels and Tg was noted with increasing ratio of the hydrophilic component (NaAlg) in samples feed composition (VNa-2, VNa-3). This is because the addition of NaAlg increases the hydrophilicity of the gel network, leading to a decrease in the hydrophobic engagements between chains of polymer blend, increasing Tso-gels and Tg. On the other hand, it was noted that the Tso-gels and Tg decreased as the thermoresponsive component (NVCL) concentration increased (VNa-4, VNa-5, VNa-6). This is because of successive hydrophobic contacts of the carbon chains of NVCL that resulted in the decreased Tso-gels and Tg. Figure 1 refers to phase transition of PNVCL/NaAlg

**Table 2.** Clarity of PNVCL/NaAlg pH/thermoresponsive hydrogels and retrieved IBP contents (%) (Mean  $\pm$  SD).

Formulations	Clarity	Drug Contents %
NVa-1	+++++	–
NVa-2	+++++	–
NVa-3	+++++	–
NVa-4	+++++	$95 \pm 1$
NVa-5	+++++	$87 \pm 1$
NVa-6	++++	$83 \pm 1$

Clarity; Good; +++++, Fair; +++++.

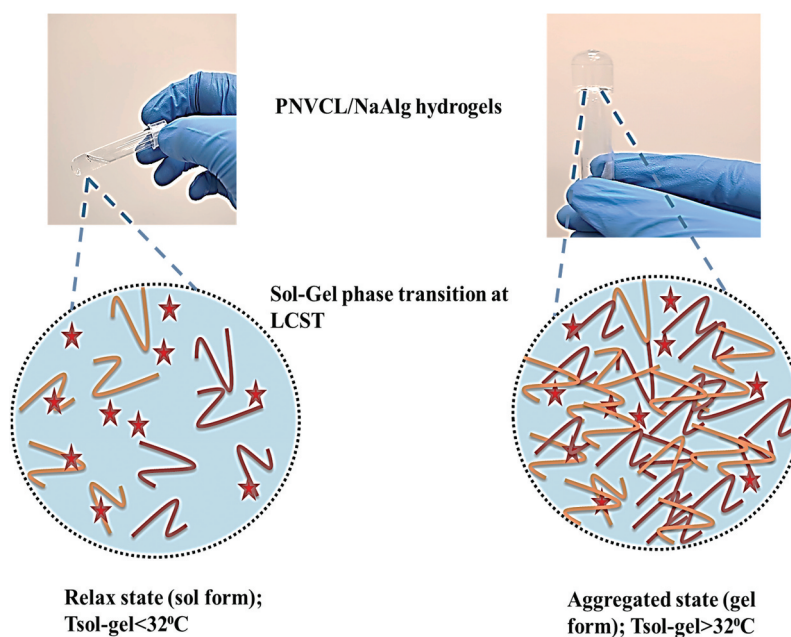


**Figure 1.** Phase change of PNVCN/NaAlg *in situ* formed pH/thermoresponsive hydrogels from sol to gel above and below LCST.

pH/thermoresponsive hydrogels from relax (sol) state to an aggregated (gel) state below and above LCST.

### 3.3. Rheological analysis

The storage ( $G'$ ) and loss moduli ( $G''$ ), which define the thixotropic properties and stable nature of hydrogel samples, were evaluated using a variety of experiments in order to monitor the strength or stability and validate the gelation of *in situ* formed hydrogels at body temperature.

#### 3.3.1. Time sweep test

Important considerations for *in situ* produced injectable hydrogels as drug delivery depots include appropriate mechanical strength and stability in physiological settings. An injectable depot system's syringibility, drug mixing ability, and release profile are all closely related to its rheological behavior.

Time sweep tests were conducted at 30°C using an AR2000 rheometer in oscillatory mode to study the detailed gelation process. The crossover point is thought to be a key point for phase change of *in situ* formulated hydrogels, where the loss (viscous) modulus ( $G''$ ) passes the storage (elastic) modulus ( $G'$ ) with time elution. For every hydrogel sample, it was found that the initial ( $G''$ ) was higher, indicating the materials' sol condition. The storage modulus ( $G'$ ) grew more quickly with time elution than the initial ( $G''$ ) modulus, with each gel sample having a gelation point that corresponded to the sol-gel transition. The

samples were in their gel condition at this transition point, where  $G' > G''$  denotes the predominate elastic phase. Moreover, NVCL increasing ratio effect on gelation response and time elution was also studied. It was noted that as NVCL contents were increased, the  $G'$  dominated the  $G''$  more quickly, and crossover points were observed at earlier time points at 105 seconds and 95 seconds respectively for these samples. This was observed because of the increased ratio of NVCL, resulting in increased hydrophobicity of network, leading to quicker aggregation and gelation. Figure 2a–c refers to oscillatory time sweep data indicating changes in  $G'$  and  $G''$  values of PNVCN/NaAlg thermoresponsive hydrogels with reaction time.

#### 3.3.2. Temperature sweep test

The values of the  $G''$  and  $G'$  were assessed throughout a wide temperature range in response to the temperature change of the circulating water bath attached to the AR2000 rheometer. Results indicated that the PNVCN/NaAlg hydrogels did not exhibit sol-gels change across the temperature range (20–45°C) at 0.5 g concentration of NVCL in the formulations. At the beginning of the experiment, higher values of  $G''$  were seen; however, as the temperature increased, the hydrophobic entanglements and NVCL's carbon chain aggregation dominated, resulting in sol-gel change of hydrogels. This rise in  $G'$  was brought on by a temperature shift related to formulations gel state. Figure 2d refers to changes in  $G'$  and  $G''$  of PNVCN/NaAlg thermoresponsive hydrogels under diverse temperature changes of the circulating water bath.

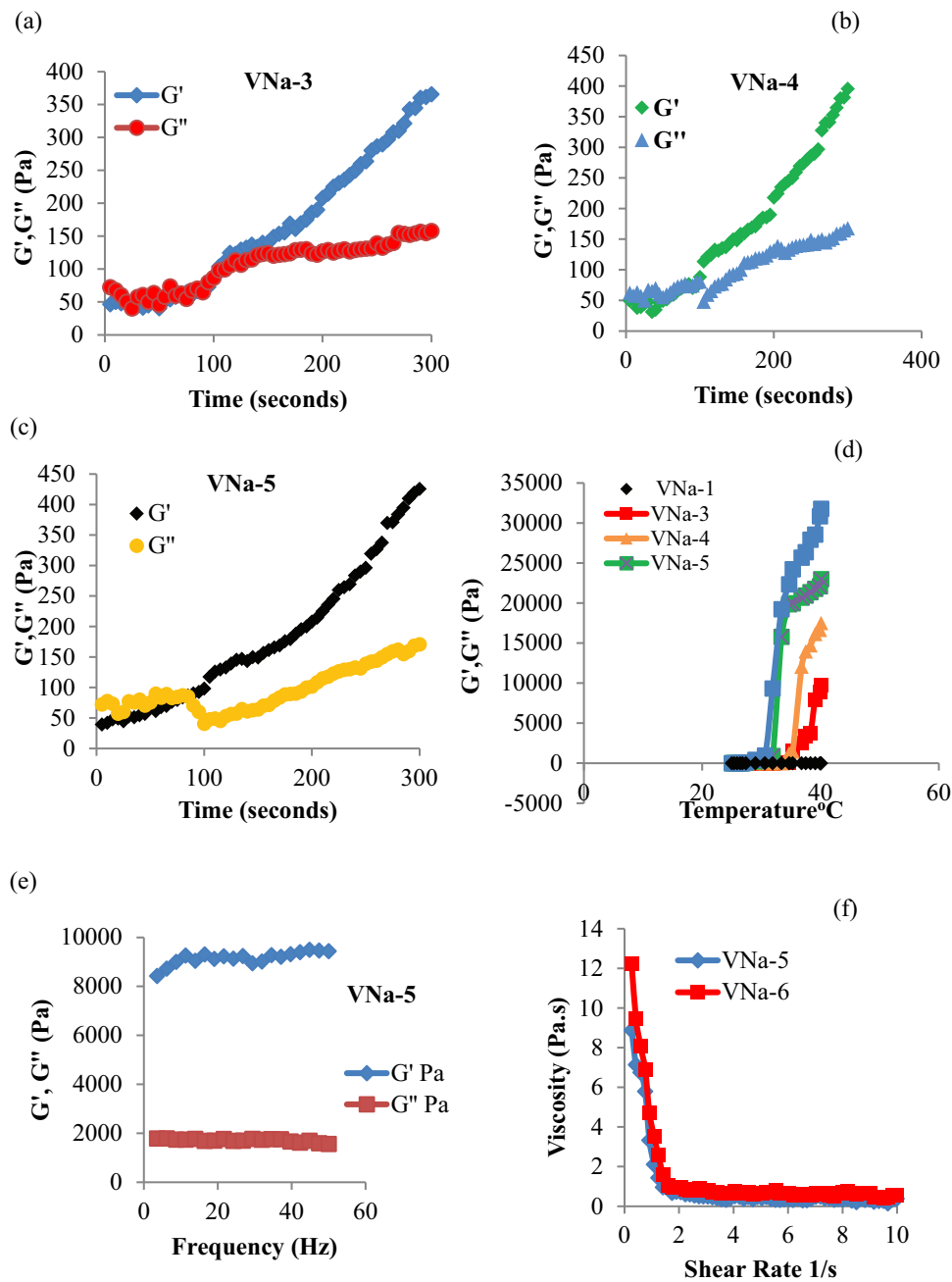


**Figure 2.** Time sweep oscillatory analysis of PNVCL/NaAlg thermoresponsive hydrogels at 30 $^{\circ}\text{C}$  for 300 seconds at controlled strain and frequency (a, b, c). Changes in  $G''$  and  $G'$  of PNVCL/NaAlg hydrogels over 20–40 $^{\circ}\text{C}$  by temperature sweep analysis (d). Stability of PNVCL/NaAlg depot hydrogels by frequency sweep analysis under controlled strain (1%) (e). Viscosity change of PNVCL/NaAlg hydrogels under 0.1–10  $\text{s}^{-1}$  shear rate. Results showed ( $n = 3$ ).

### 3.3.3. Frequency sweep test

The mechanical spectrum of PNVCL/NaAlg thermoresponsive injectable hydrogels is described by the frequency sweep test, performed under controlled strain conditions of 1% and measures changes in  $G'$  and  $G''$  with frequency variation under 0.01–50 Hz. As per results obtained,  $G'$  values were greater than  $G''$ , which indicates that PNVCL/NaAlg thermoresponsive injectable hydrogels had a stable structure above the

LCST. Figure 2e indicates the effect of variable frequency on  $G'$  and  $G''$  values of PNVCL/NaAlg thermoresponsive hydrogels.

### 3.3.4. Continuous ramp test

PNVCL/NaAlg thermoresponsive injectable hydrogels thixotropic characteristic was examined using a continuous ramp test that increased shear rate between 0.1 and 10

$s^{-1}$  over ten minutes. It was discovered that all samples demonstrated a progressive reduction in viscosity at room temperature as a function of increased shear rate. This suggests that shear thinning property of gels is related to the breaking down of crosslinks between the groups with increase in the applied force. Figure 2f indicates the changes in viscosity as a function of increasing shear rate.

### 3.4. Transparency assessment of PNVCL/NaAlg thermoresponsive hydrogels

To verify the phase transition at physiological temperature, another parameter to be monitored is the shift in optical transparencies of PNVCL/NaAlg thermoresponsive hydrogels. The optical transmittances were measured at low and high LCST of hydrogel samples. It was discovered that the polymer blend solution was clear, uniform and colorless at the beginning of the experiment. Their uniform nature, however, quickly altered as the temperature raised gradually. It was discovered that all of samples showed a sharp shift in transparencies with rising temperatures above the LCST, becoming rather opaque around 33°C. These optical transmittance studies verified that the gels' LCST was close to body temperature. Figure 3a refers to temperature-induced changes in optical transmittances of PNVCL/NaAlg pH/thermoresponsive hydrogels.

### 3.5. *In vitro* degradation

In addition of diffusion based release mechanism, drug release from hydrogel network also depends on the degradation of the polymeric network. Hydrolysis-induced

random chain cutting is the primary cause of surface degradation, as seen by the degradation profile of PNVCL/NaAlg hydrogels. As illustrated in Figure 3b, the *in vitro* degradation profile revealed that PNVCL/NaAlg hydrogels have a regulated breakdown rate at 37°C. Gel samples that had greater polymeric contents (VNa-5, VNa-6) showed the weight loss for longer time period. This degrading mechanism stabilizes the mechanical characteristics of the hydrogels while providing controlled long-term drug release.

### 3.6. Swelling study

PNVCL/NaAlg pH/thermoresponsive hydrogels were subjected to swelling investigations at varying temperature in sealed containers using pH 7.4 and pH 1.2.

#### 3.6.1. Effect of pH on swelling profile

PNVCL/NaAlg hydrogels' pH-dependent equilibrium swelling ratio was ascertained by performing swelling experiments in different pH mediums. The highest swelling ratio for the PNVCL/NaAlg hydrogels was observed in PBS (7.4) at 35°C. This was because the (–COO) groups in NaAlg remain ionized in basic fluids, which resulted in chain repulsion and caused the gel network to swell. In addition, ionized groups changes to the deionized state in pH 1.2. The gel network's repulsive forces were eliminated by this group deionization, which lowered the swelling ability of hydrogels. In acidic environment, hydrogels exhibited limited swelling behavior. However, some swelling of hydrogels was noted which attributes to solvent diffusing into the hydrogel network due to presence of hydrophilic

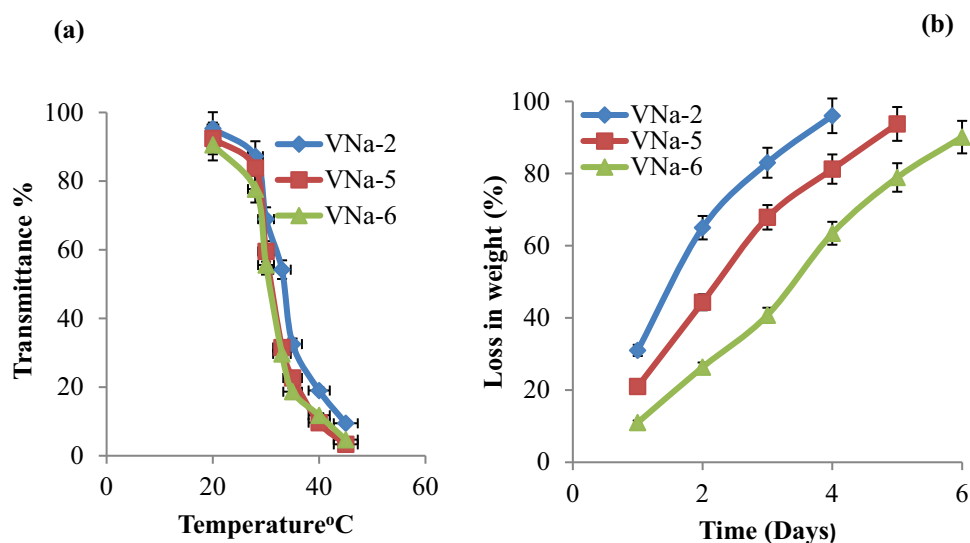


**Figure 3.** Temperature-induced changes in optical transmittances of PNVCL/NaAlg pH/thermoresponsive hydrogels (a) *In vitro* degradation analysis of PNVCL/NaAlg pH/thermoresponsive hydrogels at 37°C. Results displayed ( $n = 3$ ).



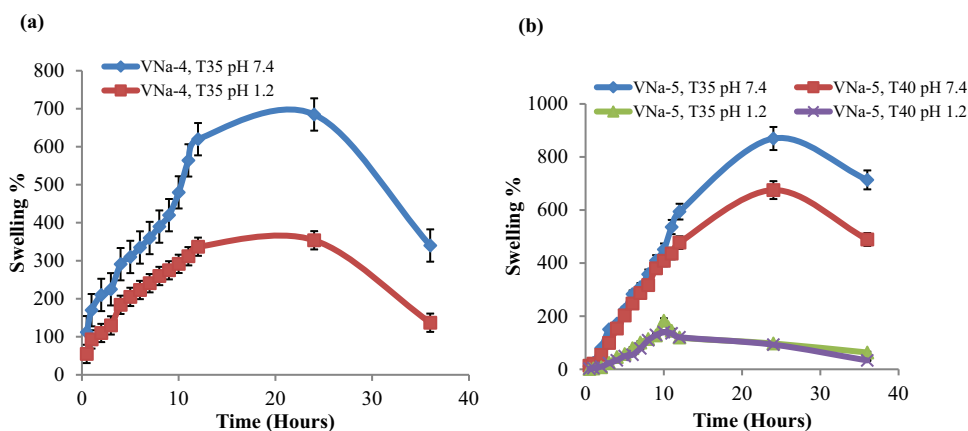


**Figure 4.** Response of PNVL/NaAlg pH/thermoresponsive hydrogels to pH change of swelling media at 35°C (a) pH and temperature effect on swelling response of PNVL/NaAlg pH/thermoresponsive hydrogels at different temperatures (35°C and 40°C) and in varied swelling media (b).

groups in hydrogels structure. Additionally, hydrogels showed decrease in swelling after 24 hours. This is suggested because, as PNVL/NaAlg hydrogels are physically entangled and the solvent is diffused inside gel network. However, after saturation of gel network, the physical interactions between polymer groups started breaking that in turn lead to gel network breakage, escape of solvent and reduced swelling. Figure 4a shows the pH sensitive behavior of PNVL/NaAlg pH/thermoresponsive hydrogels at constant temperature.

### 3.6.2. Effect of temperature on swelling profile

Temperature dependent swelling experiments were conducted in variable swelling media at two distinct temperatures (35°C and 37°C) in order to evaluate the temperature-dependent swelling behavior. It was found that at 35°C, the hydrogels showed the fastest and highest swelling ratio. This was because at 35°C, hydrogels remained in relax state leading to enhanced water uptake and swelling is resulting from forming an intermolecular entanglement between hydrophilic (-CONH-) groups of PNVL and NaAlg with the surrounding water moieties. The hydrogen bonds that hold water molecules and the gel network together, however, dissolve as the temperature upsurges above the LCST (40°C). The transition of water moieties from their bound state to their free state causes the water moieties to be removed from gel network, reducing the swelling. Figure 4b indicates the effect of pH and temperature on swelling profile of PNVL/NaAlg pH/thermoresponsive hydrogels at two different temperatures.

## 3.7. Retrieved drug contents

PNVL/NaAlg hydrogels loaded with IBP (200 ug/ml) were saturated in PBS (pH = 7.4) at 37°C for 24 hrs. Aliquots were taken and evaluated for drug contents using UV-1601 spectrophotometer (Shimadzu) at 220 nm. Table 2 entitles the IBP contents released from PNVL/NaAlg pH/thermoresponsive hydrogels at constant temperature.

## 3.8. Invitro drug release

Franz diffusion cell setup was used to test *in vitro* IBP release from PNVL/NaAlg hydrogels at  $37 \pm 2^\circ\text{C}$  and at pH 1.2 and 7.4. Selected IBP-loaded PNVL/NaAlg pH/thermo-responsive hydrogel samples were used to study the effects of various parameters.

### 3.8.1. Effect of pH on IBP release

One significant factor influencing drug release encapsulated in hydrogel matrix is the pH of the surrounding media. The release profile of PNVL/NaAlg hydrogel revealed that the hydrogel exhibited the highest IBP release at 7.4. This is because, in basic conditions, (-COO) groups in the gel network ionize, causing an electrostatic repulsion between the gels network. This opposing pressure causes the chains to relax, which opens the pores. These holes serve as pathways for the release of the IBP encapsulated within the gel matrix and the diffusion of solvent molecules within the system. The hydrogel release

profile indicated that more than 90% of the drug released from hydrogel sample within 24 hours.

As compared to pH 7.4, a reduced amount of drug was released in the media of pH 1.2. This is because of the fact that when the carboxylate groups ( $-\text{COO}^-$ ) in an acidic environment deionize, it leads to the removal of repulsive forces from the gel network and in turn, deswelling occurs and a reduction in IBP release is observed. However, some IBP release does occur in acidic conditions, which may be explained by the drug's concentration gradient and release caused by some solvent molecules uptake owing to hydrophilic groups presence. Figure 5a depicts the pH effect on IBP release from PNVCL/NaAlg pH/thermo responsive hydrogels at constant temperature.

### 3.8.2. Effect of NVCL on IBP release

Three hydrogel samples with different NVCL ratios (VNa-4, VNa-5 and VNa-6) of PNVCL/NaAlg hydrogels were formulated to investigate the impact of NVCL contents on IBP release. As the amount of NVCL in the gel compositions increased, release profile showed that release of the drug was reduced. This is suggested because of the fact that as NVCL possesses hydrophobic carbon chain, and as its ratio increased in structure, so do hydrophobic moieties. On the other hand, this causes the network to aggregate

owing to most hydrophobic interactions. This network structure aggregation subsequently slows down the drug's release. Figure 5b refers to the effect of NVCL contents on IBP release from PNVCL/NaAlg pH/thermo responsive hydrogels at constant temperature.

#### 3.8.2.1. Drug release kinetics

The regression coefficient ( $R^2$ ) values near 1 were taken into consideration when choosing the best model. Table 3 indicates the drug release kinetics of PNVCL/NaAlg hydrogels (VNa-4) at 37°C. Results indicate the VNa-4 followed zero model kinetics with  $R^2$  value close 1. The release kinetics show that the drug was released by a pore diffusion mechanism, independent of the drug concentration at the application site. The release mechanism was predicted using the Korsmeyer-Pappas model. The release exponent 'n' values showed that all of the samples followed non-Fickian diffusion, with 'n' values greater than 0.5.

### 3.9. Cytotoxic potential of PNVCL/NaAlg hydrogels

The MTT assay was applied to evaluate the cytotoxicity and cytocompatibility of PNVCL/NaAlg hydrogels. Unloaded and IBP-loaded PNVCL/NaAlg hydrogels were evaluated for safety against L929 cells (mouse fibroblast cell lines). Triton X-100 treated and unattended cells were

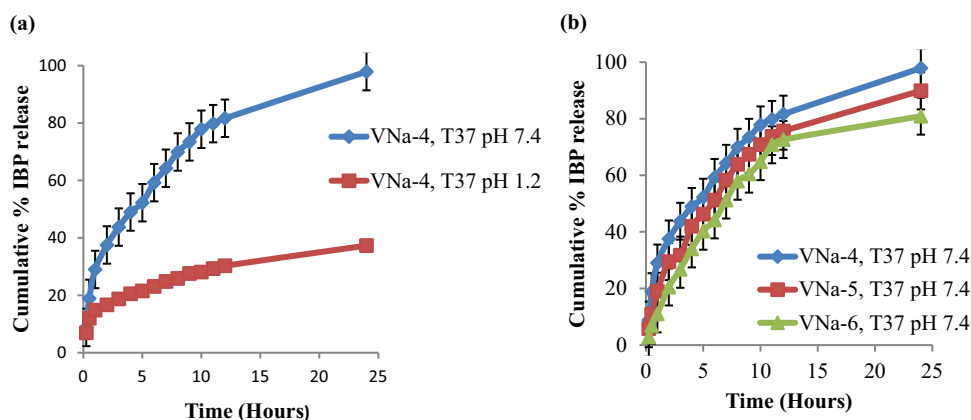


**Figure 5.** Effect of pH on invitro IBP release from pH/thermo dual responsive PNVCL/NaAlg hydrogels at 37°C (a) effect of NVCL contents on IBP release from PNVCL/NaAlg hydrogels at 37°C (b) results showed (mean  $\pm$  SD,  $n = 3$ ).

**Table 3.** Drug release kinetics.

Sample	pH	Zero order		First order		Higuchi Model		Korsmeyer–Peppas	
		$K_0$	$R^2$	$K_1$	$R^2$	$K_H$	$R^2$	n	$R^2$
VNa-4	7.4	1.35	0.999	0.076	0.991	7.48	0.984	0.579	0.989
	1.2	1.53	0.992	0.052	0.990	9.34	0.991	0.595	0.984

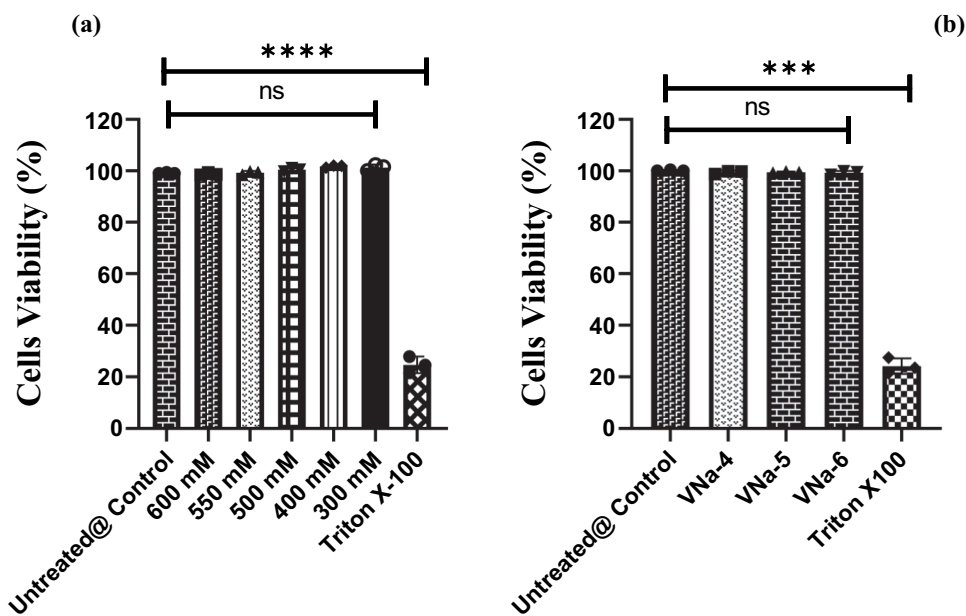


**Figure 6.** *In vitro* cytocompatibility of blank pH/thermo dual responsive PNVC/NaAlg hydrogels at varied concentrations against L929 cells in comparison to unattended and triton-x100 applied cells,  $***p = 0.0001$  (a) cytocompatibility of IBP loaded pH/thermo dual responsive PNVC/NaAlg hydrogels against L929 cells,  $**p = 0.001$ .

used as positive and negative controls respectively. Figure 6a,b revealed that, in contrast to untreated cells, blank and IBP loaded (200  $\mu\text{g}/\text{ml}$ ) gel samples displayed cell viability of above 90% at all concentrations. In contrast, cells applied with Triton-X 100 displayed cell death due to its toxic nature. These results showed that optimized IBP loaded PNVC/NaAlg hydrogels are safe and nontoxic and can be utilized as drug carrier and controlled drug depot via injectable route.

### 3.10. FTIR analysis

FTIR analysis proved the structural modifications of NaAlg and NVCL as well as the effective interactions of the two compounds. FTIR spectra of pure components and gel sample (VNa-4) have been depicted in Figure 7. Pure NaAlg's FTIR displayed in Figure 7a revealed large peak at  $3290\text{ cm}^{-1}$  attributed to the -OH stretching groups. The stretching vibration of C-H group was related to the peak

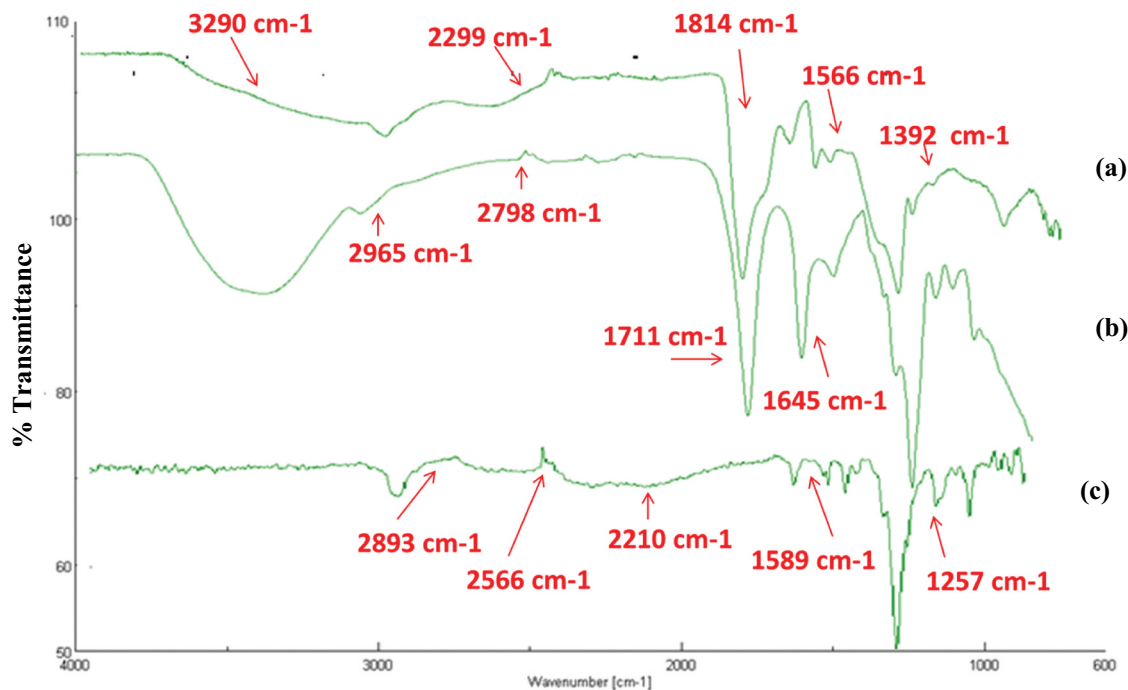


**Figure 7.** FTIR spectra of pure NaAlg (a) pure NVCL (b) freeze-dried hydrogel sample (VNa-4) (c).

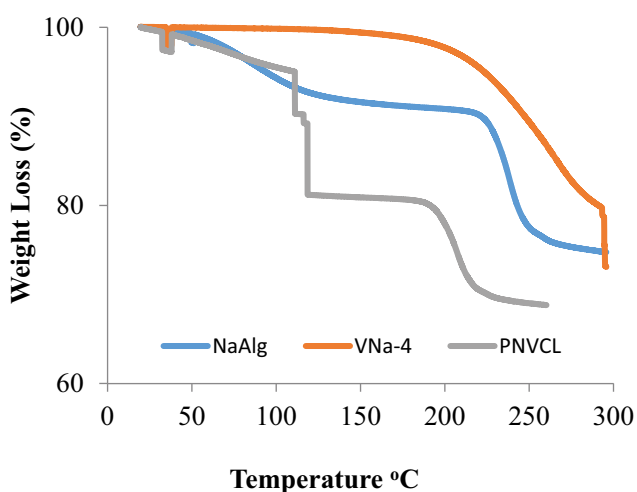


**Figure 8.** TG analysis of pure NaAlg, pure NVCL and freeze-dried hydrogel sample (VNa-4).

at  $2299\text{ cm}^{-1}$ . The peak at  $1814\text{ cm}^{-1}$  was attributed to  $\text{-COOCH}_3$  group, which resulted in the  $\text{-C=O}$  stretching. Peaks at  $1566\text{ cm}^{-1}$  and  $1392\text{ cm}^{-1}$  show Chissoring of  $\text{-CH}_2$  and bending vibrations of  $\text{-OH}$  groups respectively. Peaks at  $1210\text{ cm}^{-1}$  indicated that  $\text{-CH-OH}$  groups were present. Stretching of  $\text{-CH-O-CH-}$  appeared at  $1030\text{ cm}^{-1}$ .

The distinctive carbonyl peak at  $1645\text{ cm}^{-1}$  in pure NVCL shown in Figure 7b was attributed to  $\text{C=O}$  stretching. The  $\text{C=C}$  stretching was related to the peak at  $1711\text{ cm}^{-1}$ .  $\text{-CH}$  aliphatic stretching appeared at  $2965\text{ cm}^{-1}$  and  $2798\text{ cm}^{-1}$ . At  $1444\text{ cm}^{-1}$ ,  $\text{-CH}_2$  peak was detected. At  $2898\text{ cm}^{-1}$  and  $989\text{ cm}^{-1}$ , vinyl peaks were implicated. The stretching vibration of  $\text{C-N}$  occurred at  $1512\text{ cm}^{-1}$ .

FTIR spectra of hydrogel sample as shown in Figure 7c indicate the reduction in peak intensity at  $1589\text{ cm}^{-1}$  and  $1257\text{ cm}^{-1}$ , which may be allocated to physical contact between NaAlg and PNvCL groups. The

consumption of H-bonds was suggested by the removal of the tiny peak in the PNvCL and the shift of  $\text{C=O}$  in the  $2566\text{ cm}^{-1}$  and  $2893\text{ cm}^{-1}$  regions. The broad  $\text{C=O}$  peak seen between  $1767$  and  $2210\text{ cm}^{-1}$  is suggested to be caused by the formation of a new link between amide groups of PNvCL and  $\text{-OH}$  group of NaAlg.

### 3.11. TG analysis

NVCL showed an early rapid weight loss at decomposition temperature ( $T_d$ ) around  $33^\circ\text{C}$ , indicating the temperature sensitivity of the pure component. This degradation is thought to be caused by the evaporation of moisture, based on the TG thermograms displayed in Figure 8. Total weight loss of NVCL was observed around  $110^\circ\text{C}$  and  $119^\circ\text{C}$  respectively referring to the liberation of entrapped moisture. Pure NaAlg TG profile revealed an early weight loss at  $T_d$  between  $56^\circ\text{C}$  and  $199^\circ\text{C}$ , which was assigned to evaporation of moisture followed by degradation. The breakdown of  $\text{C-O-C}$  bonds and dehydration of saccharide rings in the NaAlg chain is considered to be the reasons for this intricate breakdown process. From the TG profile of the hydrogel sample (VNa-4), initial degradation was observed around  $34^\circ\text{C}$  confirming the presence of thermosensitive moieties in hydrogel structure. The complete degradation occurred till  $145^\circ\text{C}$ . It was observed that as the temperature was increased, the hydrogel structure was degraded due to the sudden evaporation of physically interrelated water moieties and breaking of physical links that hold gel network chains together.

### 3.12. SEM analysis

Figure 9 shows the cross-sectional morphology of PNvCL/NaAlg hydrogels. Morphology of the gels

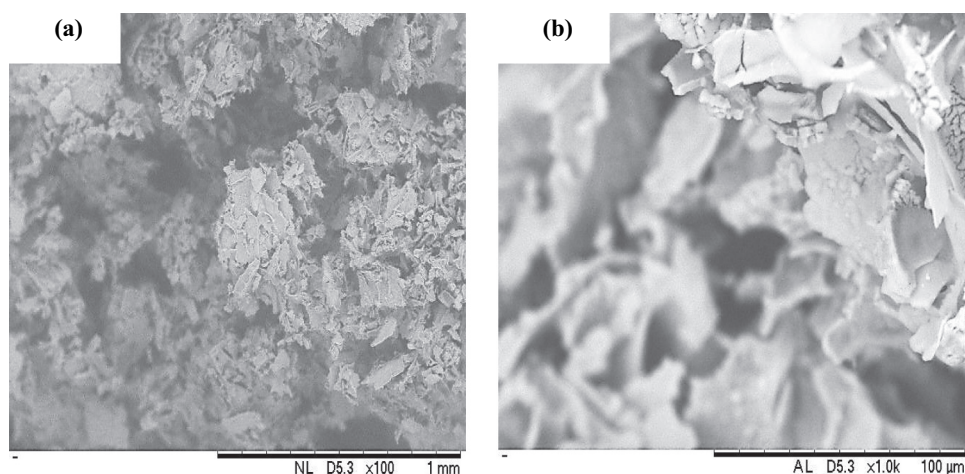


**Figure 9.** Cross-sectional morphology of freeze-dried hydrogel sample (VNa-4) at (a) magnification  $\times 100$  (b) magnification  $\times 1\text{K}$ .

revealed a highly porous complex. It has been observed and reported that such porous channels facilitate the drug diffusion across the gel network as well as facilitate the diffusion of solvent inside the polymeric network resulting in significant swelling.

#### 4. Conclusion

The current study reported the fabrication of biocompatible pH/thermoresponsive depot gel based on N-vinyl caprolactam and sodium alginate for controlled delivery of IBP. Rheological analysis confirmed that the optimized hydrogel samples possessed viscoelastic properties and exhibited a phase transition temperature from solution to gel state between 32°C and 37°C. A frequency sweep test confirmed the mechanical stability of hydrogel and could be used as a drug depot. Optical transmittance analysis revealed thermo-induced changes due to the presence of NVCL in the hydrogel structure. *In vitro* degradation analysis confirmed that optimized hydrogels have a controlled degradation rate in a basic environment (pH = 7.4). From the swelling and *in vitro* drug release profile of hydrogels, it was concluded that PNVCL/NaAlg hydrogels have both pH/thermoresponsive properties in varied environmental conditions. Maximum swelling and IBP release were observed at pH 7.4 and 35°C, assigned to the relaxed gel phase. It was also observed that PNVCL has a principal effect in gel aggregation with increasing temperature that in turn showed effect on drug release from hydrogel. MTT assay showed that optimized blank and IBP-loaded PNVCL/NaAlg hydrogels were safe and biocompatible against L929 cells and can be utilized as drug delivery carrier. FTIR analysis confirmed the polymer blend hydrogel formation, while TGA results of hydrogels showed the appearance of a thermogram between 32°C and 37°C, confirming the presence of a thermoresponsive component. SEM showed the porosity of synthesized hydrogels. In conclusion, the designed biocompatible PNVCL/NaAlg pH/thermoresponsive hydrogels can serve as depots for the controlled delivery of IBP following subcutaneous administration. Since these hydrogels showed pH/thermo dual responsive nature, however, the low swelling and drug release at low pH (1.2) was encountered the major limitation of the study.

#### Acknowledgments

The authors would like to acknowledge Margalla Institute of Health Sciences Islamabad Pakistan and the Faculty of Pharmacy Soochow University, Suzhou, China for providing lab facilities.

Also, the authors extend their appreciation to the Researchers Supporting Project number (RSPD2025R1118) King Saud University, Riyadh, Saud Arabia.

#### Disclosure statement

No potential conflict of interest was reported by the author(s).

#### Funding

Researchers Supporting Project number [RSPD2025R1118] King Saud University, Riyadh, Saud Arabia.

#### Author's contribution

Conceptualization, writing the original draft, formal analysis, investigations, data curation, software: Samiullah Khan, Abdur Rehman, Syed Faisal Badshah. investigations, resources, project administration, reviewing, and editing: Gamal A. Shazly, Amira Metouekel, Fakhredeen Dabiellil.

#### Data availability statement

All data generated or analyzed during this study are included in this published article.

#### References

- [1] Khan S, Anwar N. Gelatin/Carboxymethyl cellulose-based stimuli-responsive hydrogels for controlled delivery of 5-fluorouracil, development, in vitro characterization, in vivo safety and bioavailability evaluation. *Carbohydr Polym.* 2021;257:117617. doi: [10.1016/j.carbpol.2021.117617](https://doi.org/10.1016/j.carbpol.2021.117617)
- [2] Khan S, Minhas MU, Ahmad M, et al. Self-assembled supramolecular thermoreversible  $\beta$ -cyclodextrin/ethylene glycol injectable hydrogels with difunctional Pluronic® 127 as controlled delivery depot of curcumin. Development, characterization and in vitro evaluation. *J Biomater Sci, Polym Ed.* 2018;29(1):1–34. doi: [10.1080/09205063.2017.1396707](https://doi.org/10.1080/09205063.2017.1396707)
- [3] Kulkarni RV, Sa B. Polyacrylamide-grafted-alginate-based pH-sensitive hydrogel beads for delivery of ketoprofen to the intestine: in vitro and in vivo evaluation. *J Biomater Sci, Polym Ed.* 2009;20(2):235–251. doi: [10.1163/156856209X404514](https://doi.org/10.1163/156856209X404514)
- [4] Mather PT. Soft answers for hard problems. *Nat Mater.* 2007;6(2):93–94. doi: [10.1038/nmat1834](https://doi.org/10.1038/nmat1834)
- [5] Khan S, Akhtar N, Minhas MU. Fabrication, rheological analysis, and in vitro characterization of in situ chemically cross-linkable thermogels as controlled and prolonged drug depot for localized and systemic delivery. *Polym Adv Technol.* 2019;30(3):755–771. doi: [10.1002/pat.4514](https://doi.org/10.1002/pat.4514)
- [6] Cristiano MC, Mancuso A, Giuliano E, et al. EtoGel for intra-articular drug delivery: a new challenge for joint

- diseases treatment. *J Funct Biomater*. 2021;12(2):34. doi: [10.3390/jfb12020034](https://doi.org/10.3390/jfb12020034)
- [7] Wang W, Zhang Q, Zhang M, et al. A novel biodegradable injectable chitosan hydrogel for overcoming post-operative trauma and combating multiple tumors. *Carbohydr Polym*. 2021;265:118065. doi: [10.1016/j.carbpol.2021.118065](https://doi.org/10.1016/j.carbpol.2021.118065)
- [8] Ohya Y. Temperature-responsive biodegradable injectable polymer systems with conveniently controllable properties. *Polym J*. 2019;51(10):997–1005. doi: [10.1038/s41428-019-0217-0](https://doi.org/10.1038/s41428-019-0217-0)
- [9] Miao T, Fenn SL, Charron PN, et al. Self-healing and thermoresponsive dual-cross-linked alginate hydrogels based on supramolecular inclusion complexes. *Biomacromolecules*. 2015;16(12):3740–3750. doi: [10.1021/acs.biomac.5b00940](https://doi.org/10.1021/acs.biomac.5b00940)
- [10] Khan S, Akhtar N, Minhas MU, et al. pH/thermo-dual responsive tunable in situ cross-linkable depot injectable hydrogels based on poly (N-isopropylacrylamide)/carboxymethyl chitosan with potential of controlled localized and systemic drug delivery. *AAPS PharmSciTech*. 2019;20(3):1–16. doi: [10.1208/s12249-019-1328-9](https://doi.org/10.1208/s12249-019-1328-9)
- [11] Hu J, Chen Y, Li Y, et al. A thermo-degradable hydrogel with light-tunable degradation and drug release. *Biomaterials*. 2017;112:133–140. doi: [10.1016/j.biomaterials.2016.10.015](https://doi.org/10.1016/j.biomaterials.2016.10.015)
- [12] Macchione MA, Guerrero-Beltrán C, Rosso AP, et al. Poly (N-vinylcaprolactam) nanogels with antiviral behavior against HIV-1 infection. *Sci Rep*. 2019;9(1):5732. doi: [10.1038/s41598-019-42150-9](https://doi.org/10.1038/s41598-019-42150-9)
- [13] Montes JÁ, Ortega A, Burillo G. Dual-stimuli responsive polymer blends based on N-vinylcaprolactam/chitosan. *J Radioanal Nucl Chem*. 2015;303:2143–2150. doi: [10.1007/s10967-014-3805-7](https://doi.org/10.1007/s10967-014-3805-7)
- [14] Spěváček J, Dybal J, Starovoytova L, et al. Temperature-induced phase separation and hydration in poly (N-vinylcaprolactam) aqueous solutions: a study by NMR and IR spectroscopy, SAXS, and quantum-chemical calculations. *Soft Matter*. 2012;8(22):6110–6119. doi: [10.1039/c2sm25432h](https://doi.org/10.1039/c2sm25432h)
- [15] Hanyková L, Spěváček J, Radecki M, et al. Structures and interactions in collapsed hydrogels of thermoresponsive interpenetrating polymer networks. *Colloid Polym Sci*. 2015;293(3):709–720. doi: [10.1007/s00396-014-3455-x](https://doi.org/10.1007/s00396-014-3455-x)
- [16] Tan R, She Z, Wang M, et al. Thermo-sensitive alginate-based injectable hydrogel for tissue engineering. *Carbohydr Polym*. 2012;87(2):1515–1521. doi: [10.1016/j.carbpol.2011.09.048](https://doi.org/10.1016/j.carbpol.2011.09.048)
- [17] Swamy BY, Chang JH, Ahn H, et al. Thermoresponsive N-vinyl caprolactam grafted sodium alginate hydrogel beads for the controlled release of an anticancer drug. *Cellulose*. 2013;20(3):1261–1273. doi: [10.1007/s10570-013-9897-3](https://doi.org/10.1007/s10570-013-9897-3)
- [18] Manoukian MAC, Migdal CW, Tembhekar AR, et al. Topical administration of ibuprofen for injured athletes: considerations, formulations, and comparison to oral delivery. *Sports Med - Open*. 2017;3(1):1–9. doi: [10.1186/s40798-017-0103-2](https://doi.org/10.1186/s40798-017-0103-2)
- [19] Khan S, Minhas MU. Micro array patch assisted transdermal delivery of high dose, ibuprofen sodium using thermoresponsive sodium alginate/poly (vinylcaprolactam) in situ gels depot. *Int J Biol Macromol*. 2023;252:126464. doi: [10.1016/j.ijbiomac.2023.126464](https://doi.org/10.1016/j.ijbiomac.2023.126464)
- [20] Mundargi RC, Rangaswamy V, Aminabhavi TM. A novel method to prepare 5-fluorouracil, an anti-cancer drug, loaded microspheres from poly (N-vinyl caprolactam-co-acrylamide) and controlled release studies. *Des Monomers Polym*. 2010;13(4):325–336. doi: [10.1163/138577210X509561](https://doi.org/10.1163/138577210X509561)
- [21] Nasir F, Iqbal Z, Khan JA, et al. Development and evaluation of diclofenac sodium thermoresponsive subcutaneous drug delivery system. *Int J Pharm*. 2012;439(1–2):120–126. doi: [10.1016/j.ijpharm.2012.10.009](https://doi.org/10.1016/j.ijpharm.2012.10.009)
- [22] Moreira HR, Munarin F, Gentilini R, et al. Injectable pectin hydrogels produced by internal gelation: pH dependence of gelling and rheological properties. *Carbohydr Polym*. 2014;103:339–347. doi: [10.1016/j.carbpol.2013.12.057](https://doi.org/10.1016/j.carbpol.2013.12.057)
- [23] Pentlavalli S, Chambers P, Sathy BN, et al. Simple radical polymerization of Poly(Alginate-Graft-N-Isopropylacrylamide) injectable thermoresponsive hydrogel with the potential for localized and sustained delivery of stem cells and bioactive molecules. *Macromol Biosci*. 2017;17(11):1700118. doi: [10.1002/mabi.201700118](https://doi.org/10.1002/mabi.201700118)
- [24] Geever LM, Devine DM, Nugent MJD, et al. The synthesis, characterisation, phase behaviour and swelling of temperature sensitive physically crosslinked poly (1-vinyl-2-pyrrolidinone)/poly (N-isopropylacrylamide) hydrogels. *Eur Polym J*. 2006;42(1):69–80. doi: [10.1016/j.eurpolymj.2005.09.027](https://doi.org/10.1016/j.eurpolymj.2005.09.027)
- [25] Wang B, Wu X, Li J, et al. Thermosensitive behavior and antibacterial activity of cotton fabric modified with a chitosan-poly (N-isopropylacrylamide) interpenetrating polymer network hydrogel. *Polymers*. 2016;8(4):110. doi: [10.3390/polym8040110](https://doi.org/10.3390/polym8040110)
- [26] Fang J-Y, Chen J-P, Leu Y-L, et al. The delivery of platinum drugs from thermosensitive hydrogels containing different ratios of chitosan. *Drug Deliv*. 2008;15(4):235–243. doi: [10.1080/10717540802006674](https://doi.org/10.1080/10717540802006674)
- [27] Kim Y-H, Oh T, Park E, et al. Anti-inflammatory and anti-apoptotic effects of Acer palmatum thumb. extract, KIOM-2015EW, in a hyperosmolar-stress-induced in vitro dry eye model. *Nutrients*. 2018;10(3):282. doi: [10.3390/nu10030282](https://doi.org/10.3390/nu10030282)
- [28] Khan S, Khan B, Li H. Fabrication and evaluation of smart pH/thermo dual-responsive injectable intratumoral in situ depot hydrogels for controlled 5-FU delivery. *Beni-Suef Univ J Basic Appl Sci*. 2023;12(1):117. doi: [10.1186/s43088-023-00459-5](https://doi.org/10.1186/s43088-023-00459-5)
- [29] Khan S, Akhtar N, Minhas MU, et al. A difunctional Pluronic® 127-based in situ formed injectable thermogels as prolonged and controlled curcumin depot, fabrication, in vitro characterization and in vivo safety evaluation. *J Biomater Sci, Polym Ed*. 2021;32(3):281–319. doi: [10.1080/09205063.2020.1829324](https://doi.org/10.1080/09205063.2020.1829324)

- [30] Khan S, Ranjha NM. Effect of degree of cross-linking on swelling and on drug release of low viscous chitosan/poly (vinyl alcohol) hydrogels. *Polym Bull.* 2014;71(8):2133–2158. doi: [10.1007/s00289-014-1178-2](https://doi.org/10.1007/s00289-014-1178-2)
- [31] Jalil A, Khan S, Naeem F, et al. The structural, morphological and thermal properties of grafted pH-sensitive interpenetrating highly porous polymeric composites of sodium alginate/acrylic acid polymer blends for controlled delivery of diclofenac potassium. *Des Monomers Polym.* 2017;20(1):308–324. doi: [10.1080/15685551.2016.1259834](https://doi.org/10.1080/15685551.2016.1259834)
- [32] Li Y, Tan Y, Xu K, et al. In situ crosslinkable hydrogels formed from modified starch and O-carboxymethyl chitosan. *RSC Adv.* 2015;5(38):30303–30309. doi: [10.1039/C4RA14984J](https://doi.org/10.1039/C4RA14984J)